PLANE STRAIN AND TRIAXIAL TESTS ON UNDISTURBED SAMPLES RETRIEVED FROM FAILED SLOPE DUE TO EARTHQUAKE

Jianliang DENG[1], Yukika TSUTSUMI[2], Hiroshi KAMEYA[3], Takeshi SATO[4] and Junichi KOSEKI[5]

ABSTRACT: Plane strain and triaxial compression tests were performed on softrock specimens having a sandy layer to reveal the mechanism of a slope failure in the 2004 Niigata-ken Chuetsu Earthquake. The peak and residual strengths of saturated/unsaturated specimens, which were retrieved from the in-situ slope, were reported. To simulate the effect of earthquake, cyclic loading was applied in some tests, while no significant effect could be found. Possible effects of the membrane compliance on the undrained test results were discussed.

Key Words: Triaxial compression test, thin sandy layer, slope failure, earthquake

INTRODUCTION

Extensive slope failures occurred in the Chuetsu Earthquake which struck the Mid Niigata Prefecture with Mj=6.8 on October 23 in 2004. 3,791 slopes failed with a breakdown volume of about 100 million cubic meters in an area of about 1,310 square kilometers according to the analysis results of aerial photos (MLIT, 2005).

The extensive slope failures are likely to be affected by two factors: the continuous strong rainfall before the earthquake and many large aftershocks. Before the earthquake, this area had a rainfall which was more than 100 mm/day up to 20th October, so the soil was well saturated and the ground water level was raised from the normal level. As for the second factor, after the mainshock, many large aftershocks struck this area repeatedly within about two months.

To analyze the mechanism of the slope failures in this earthquake, one slope failure located at Yokowatashi, Ojiya City near Shinano River was investigated in this study. As shown in **Figure 1**, the failed slope is 40 m wide and 70 m long with a dip angle of about 22 degrees, and its detailed conditions before failure needed more investigation. A feature of this failure is that, at the sliding plane, there existed a sandy soil layer with a thickness of 1 to 3 cm between softrock deposits consisting of silt rock, which may be easily overlooked at the time of geotechnical survey.

In this study, triaxial compression (TC) tests were performed on dummy, artificial specimens and undisturbed sandwich specimens which were retrieved from the in-situ slope. Besides the TC tests, plane strain compression (PSC) tests were performed as well.

[1] Graduate student
[2] Research associate
[3] Expert engineer
[4] Research associate
[5] Professor

Figure 1. Slope failure investigated in this study

APPARATUS, SPECIMENS AND TEST PROCEDURES

Apparatus

The apparatus used is a modified version of PSC test apparatus (Salas Monge *et al.*, 2002). As shown in **Figure 2**, to apply the intermediate principal stress in PSC test, a set of frame was used, which consisted of one stiffening steel frame, one transparent plexiglass confining plate, another confining plate, three load cells, an end plate and four tie rods. This set of frame was supported by ball bearings. If this frame is taken off, the apparatus can be used to perform TC test with a prismatic specimen. In

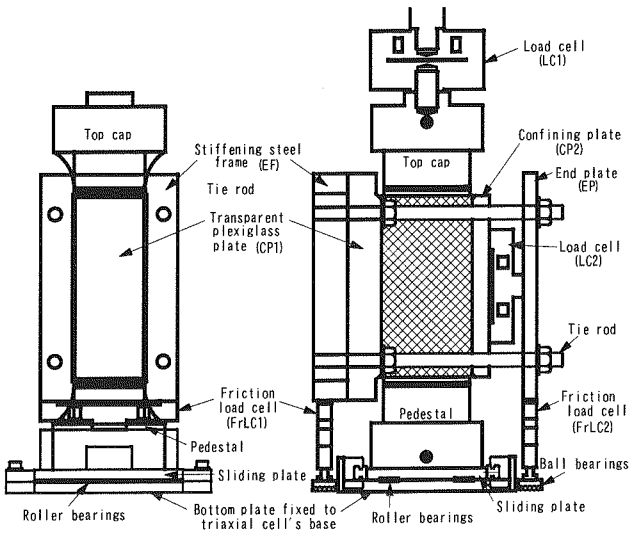

Figure 2. Test apparatus

this study, more number of TC tests than PSC tests were performed. This is because of the observation in PSC tests that the sandwiched sandy layer could not adequately touch the confining plates, which caused technical difficulty in conducting image analysis on the deformation of the sandy layer.

An external transducer was used to measure the global axial strain, and three pairs of Local Deformation Transducers (LDTs) were used to measure the deformation near the sandy layer and the deformation of softrock. The volume change was measured by a Low Capacity Differential Pressure Transducer (LCDPT), and the minor principal stress was measured by a High Capacity Differential Pressure Transducer (HCDPT).

A 0.3-mm-thick membrane was used, and dots were imprinted on the membrane at a spacing of 5 mm. A digital camera with a resolution of 8 mega pixels was used to take photos of these dots for image analysis.

Specimens and Test procedures

Three types of specimens (undisturbed block specimen, undisturbed sandwiched specimen (**Figure 3**) and artificial specimen) were used for various purposes as listed in **Table 1**. It should be noted that a series of direct shear (DS) tests were also performed on the undisturbed sandwiched specimens while the details of DS tests will be reported elsewhere (Tsutsumi *et al.*, 2007). In addition, an aluminum dummy (60x80x160 mm) was used to investigate the effects of membrane compliance.

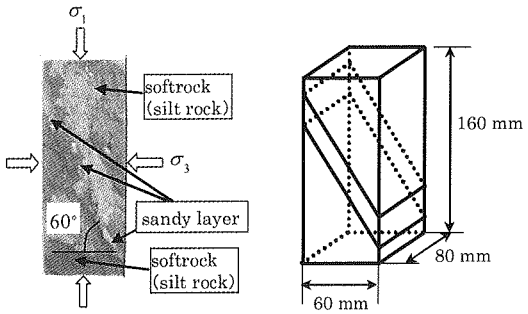

Figure 3. Undisturbed sandwiched specimen (test TC-1)

Undisturbed block specimen (60x80x160 mm, R- group) and undisturbed sandwiched specimen (60x80x160 mm, PSC- group and TC- group) were retrieved from the in-situ location. The R- group undisturbed specimens did not contain sandy layer; the PSC- group, TC- group, and DS- group specimens contained a thin sandy layer which is very weak, so the trimming procedure was performed very carefully not to alter the original condition (Kameya *et al.*, 2006). The grain size distribution of the sandy layer in specimen TC-9 is shown in **Figure 4**. The mean diameter D_{50} of the sandy layer is

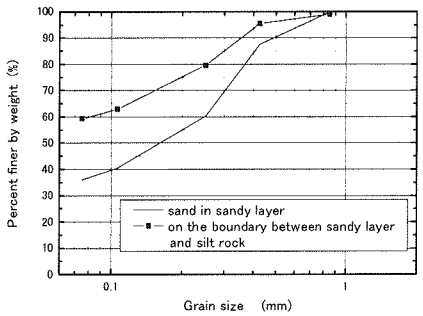

Figure 4. Grain size distribution curve of specimen TC-9

Table 1. Test conditions

test No. [1]	dry density ρ_d (g/cm^3)	water content w (%)	test type[2]	saturation condition[3]	test condition for shear[4]	B-value (%)	effective confining pressure [5] σ_3' or σ' (kPa)	deviator stress during creep q_0 (kPa)	inclina -tion of sandy layer (°)
R-1	1.44	31.0	PSC	DVS	D	67.5	*50*	-	-
R-2	1.41	30.6	PSC	DVS	UD	94.2	*54*	-	-
PSC-1	*1.30*	*34.7*	PSC	DVS	UD	*97.4*	*49*	*39*	*61.7*
TC-1	*1.36*	*33.0*	TC	DVS	UD	*86.7*	*48*	*45*	*54.4*
TC-2	*1.31*	*34.1*	TC	DVS	UD	*98.9*	*51*	*45*	*54.8*
TC-3	*1.32*	*35.1*	TC	DVS	D	*98.2*	*90*	-	*56.3*
TC-4	*1.29*	*35.6*	TC	DVS	D	*97.6*	*20*	-	*60.1*
TC-5	*1.32*	*29.0*	TC	US	D	-	*45*	-	*47.5*
TC-6	*1.33*	*29.5*	TC	US	D	-	*90*	-	*51.9*
TC-7	*1.33*	*29.8*	TC	US	D	-	*20*	-	*62.2*
TC-8	*1.33*	*33.7*	TC	DVS	UD	*98.5*	*52*	*44*	*53.1*
TC-9	*1.38*	*32.1*	TC	DVS	UD	*98.8*	*45*	*45*	*51.3*
A-1	*1.49*	-	TC	DVS	UD	*99.3*	*45*	*45*	-
A-2	*1.49*[*)]	-	TC	DVS	UD	*99.2*	*45*	*45*	*60*
A-3	*1.49*[*)]	-	TC	DVS	UD	*98.8*	*45*	*45*	*60*
DS-1	-	-	DS	S	CV	-	*50*		*0*
DS-2	-	-	DS	S	CV	-	*75*		*0*
DS-3	-	-	DS	US	CP	-	*50*		*0*
DS-4	-	-	DS	US	CP	-	*50*		*0*
DS-5	-	-	DS	US	CP	-	*25*		*0*

[1)] A-1: made of Toyoura sand;A-2 and A-3: made of Toyoura sand and softrock blocks; R-1 and R-2: made by undisturbed softrock without sandy layer; all the other specimens are undisturbed specimens with sandy layer.

[2)] PSC: Plane Strain Compression test; TC: Triaxial Compression test; DS: Direct Shear test.

[3)] DVS: Saturated by double vacuuming method; US: Unsaturated; S: saturated by submerging.

[4)] D: Drained; UD: Undrained; CV: Constant Volume; CP: Constant vertical Pressure.

[5)] σ_3' in PSC and TC, and σ' in DS before starting monotonic shear.

[*)] Dry density of Toyoura sand layer. Thickness of Toyoura sand layer: 16 mm in specimen A-2; 8 mm in specimen A-3.

0.16 mm, while the D_{50} value is less than 0.07 mm for the sandy clay which was located on the boundary between the sandy layer and the silt rock.

Artificial specimens (56x78x160 mm, A- group) made by Toyoura sand (D_{50}=0.2mm, ρ_s=2.656g/cm^3) with/without two softrock blocks were used to simulate the condition of the undisturbed sandwiched specimens and to investigate whether liquefaction can occur.

For saturated undrained test on undisturbed sandwiched specimens and artificial specimens, with a confining stress σ_3' of 30 kPa the specimens were firstly saturated by using the double vacuuming method which consists of vacuuming, flushing with de-aired water and back pressurization (Ampadu and Tatsuoka, 1993). After consolidating the specimen isotropically, drained loading was performed until the deviator stress q_1 ($=\sigma_1 - \sigma_3$) reached the prescribed value (q_0) to reproduce the in-situ stress state (Tsutsumi *et al.* 2007). After a 50-minute drained creep loading with the deviator stress q_1=q_0, undrained creep loading was applied for 10 minutes to reproduce the in-situ stress condition just before the earthquake. Finally, undrained monotonic/cyclic shearing was applied until the end of test.

In the cyclic tests on undisturbed sandwiched specimens and artificial specimens, undrained cyclic loadings with a double amplitude deviator stress, q_d, of 30, 60, 90, 120 and 150 kPa were applied step by step. At each loading step, ten cycles were applied. Finally, undrained monotonic loading was applied to the specimen.

For saturated drained test, the specimens were consolidated isotropically, and after saturation,

drained monotonic loading was applied. For unsaturated test, specimens were sheared directly after consolidation, while maintaining the initial water constant. In saturated drained test and unsaturated test, the confining stress was kept constant during shearing.

For all the saturated tests, B value was measured after saturation. For all the undisturbed specimens, dry density was measured after the tests. For artificial specimens, the dry density of sandwiched Toyoura sand was evaluated based on the calibration results employing the same air pluviation method. For all the test, during monotonic loading and cyclic loading, the strain rate was 0.16%/min when axial strain measured by external transducer ($\varepsilon_{1,EXT}$) was less than 2.5%; after the $\varepsilon_{1,EXT}$ value exceeded 2.5%, the strain rate was changed to 0.08%/min for test PSC-1, and 0.05%/min for test TC-8.

Dummy specimens were used to investigate the possible effects of membrane compliance on the test results. Three tests were performed by using an aluminum dummy specimen which was covered by 0.3-mm-thick membrane with an inner circumferential length of 283 mm. The test procedure of dummy test was as follows: first, the specimen was double vacuumed; second, water flowed into the void space which was covered by the membrane when the specimen was being double-vacuumed; then, cell pressure and back pressure were increased to 245 kPa and 200 kPa, respectively, to ensure that the space covered by the membrane was fully occupied by water; finally, while ensuring the deviator stress to be constant (-5 , 0, or 5 kPa), the cell pressure was decreased from 245 kPa to 202 kPa gradually at the constant back pressure of 200 kPa. During the last stage, the volume of water that flowed into the space covered by the membrane was recorded to obtain the relation between this water volume and effective confining stress.

For all the PSC and TC tests including dummy tests, lubrication was conducted at the interfaces between the specimen and the top cap, pedestal and confining plates (in case of PSC tests) to reduce friction, and filter paper was used at the side of the specimen to ensure saturation and possible drainage.

TEST RESULTS AND DISCUSSION

Test results on undisturbed specimens

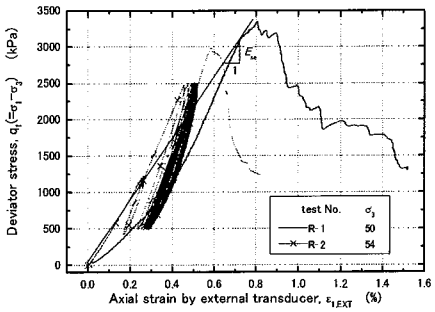

Figure 5. Stress-strain relationships of specimens without sandy layer

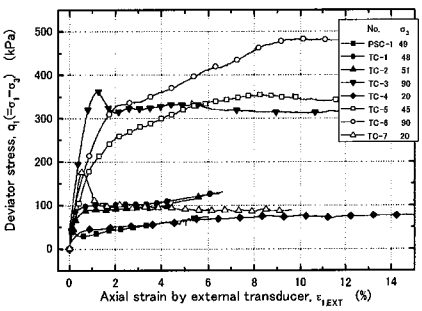

Figure 6. Stress-strain relationships of undisturbed specimens with sandy layer

Figure 5 shows that softrock specimens (R-group) under the effective confining stress of about 50 kPa exhibit the peak strength of about 3000 kPa and their corresponding secant Young's modulus E_{se} of about 450 MPa. On the other hand, with the sandwiched specimens with sandy layer (PSC-1, TC-1 and TC-2) the peak strength is 45-100 kPa, and the secant Young's modulus is about 30MPa (**Figure 6**).

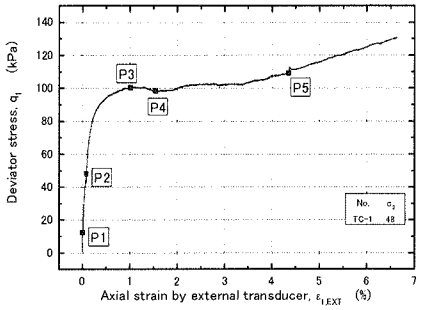

Figure 7a). Stress-strain relationship of specimen TC-1

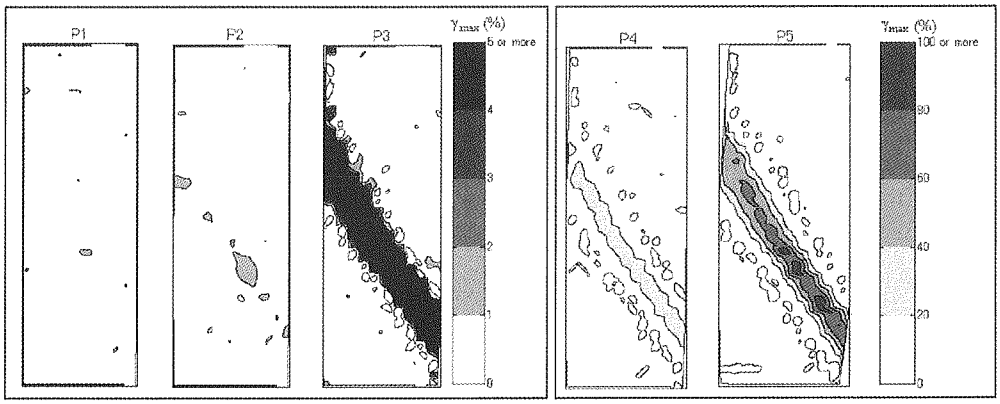

Figure 7b). Maximum shear strain distributions at the states from P1 to P5 in test TC-1

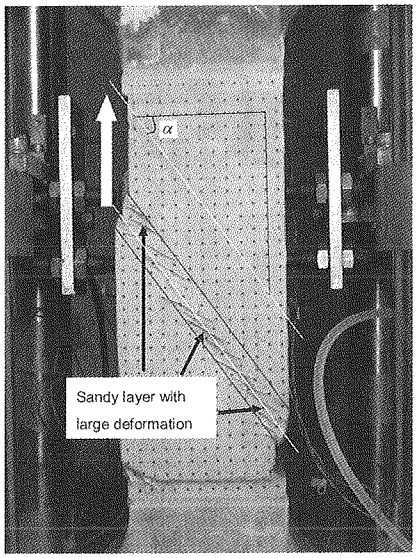

Figure 8. Evaluation of the orientation of sandy layer (test TC-1)

For the specimens with sandy layer, the strain level in the sandy layer can not be evaluated from the overall deformation. Therefore, image analysis was performed to evaluate the local strain distribution.

Figure 7 b) shows the contours of the maximum shear strain $\gamma_{max}(=\varepsilon_1-\varepsilon_3)$ which is obtained from the displacement of dots imprinted on the membrane. The value of γ_{max} was defined as an average for a grid of 5 mm and set to be zero at the isotropic stress state before vertical loading.

From **Figure 7**, it can be seen that, at the peak stress state P3, the sandy layer deformed predominantly, while the softrock regions exhibited much smaller deformation. At state P5, some areas in the softrock regions, such as those near the pedestal, near the top cap or near the interface with the sandy layer, the maximum shear strain exceeded 3%. Note that the membrane had obvious wrinkles in these areas, therefore the maximum shear strain distribution in these areas may not be reliable. The extensive wrinkles in these areas after shearing can be seen in **Figure 8** as well.

According to **Figure 7** and other image analysis results, it is found that deformation is concentrated into the whole part of sandy layer, while sliding failure occurred near the boundary of sandy layer and softrock at large deformation.

Figure 9 shows the effective stress path of both saturated and unsaturated tests. Considering that the sandy layer controlled the overall strength and the inclination of the sandy layer, α, varied in a large range between 47.5° to 62.2° measured from the horizontal direction (**Table 1**), the strength of sandy layer may not be compared directly based on **Figures 6** and **9**. Therefore, the ratio of shear stress to effective normal stress mobilized along the plane parallel to the direction of the sandy layer was computed as follows.

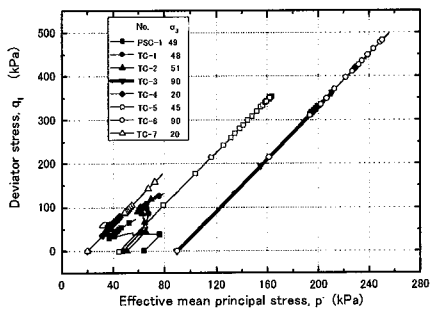

Figure 9. Stress paths of undisturbed samples with sandy layer

As the sandy layer was not always in the form of straight band as typically shown in **Figure 8**, its inclination, α, was determined by using photos taken for image analysis. First, a line was drawn to follow the average direction of the band; then, a parallel line was drawn; finally the inclination of the parallel line was evaluated referring to the imprinted points which suffered very limited relative displacements during loading. For example, the average inclination of sandy layer in **Figure 8** (specimen TC-1) is obtained as α=atan(70 mm/50.2 mm)=54.4°.

As the effective major principal stress σ_1' and the effective minor principal stress σ_3' are known, the effective normal stress σ_α' and shear stress τ_α acting on the sandy layer surface can be calculated as

$$\sigma_\alpha' = (\sigma_1' + \sigma_3')/2 + (\sigma_1' - \sigma_3')/2 \times \cos(2\times\alpha)$$
$$\tau_\alpha = (\sigma_1' - \sigma_3')/2 \times \sin(2\times\alpha)$$

The nominal shear strain mobilized along the sandy layer is evaluated based on the measured value of the volumetric strain ε_{vol} and the major principal strain ε_1, while assuming for simplicity that the

intermediate principal strain ε_2 is zero, as follows:

$$\varepsilon_{vol} = \varepsilon_1 + \varepsilon_2 + \varepsilon_3 = \varepsilon_1 + \varepsilon_3$$
$$\varepsilon_3 = \varepsilon_{vol} - \varepsilon_1$$
$$\gamma_\alpha / 2 = (\varepsilon_1 - \varepsilon_3)/2 \times \sin(2 \times \alpha)$$
$$= (\varepsilon_1 - (\varepsilon_{vol} - \varepsilon_1))/2 \times \sin(2 \times \alpha)$$
$$= (2 \times \varepsilon_1 - \varepsilon_{vol})/2 \times \sin(2 \times \alpha)$$

and thus $\gamma_\alpha = (2 \times \varepsilon_1 - \varepsilon_{vol}) \times \sin(2 \times \alpha)$.

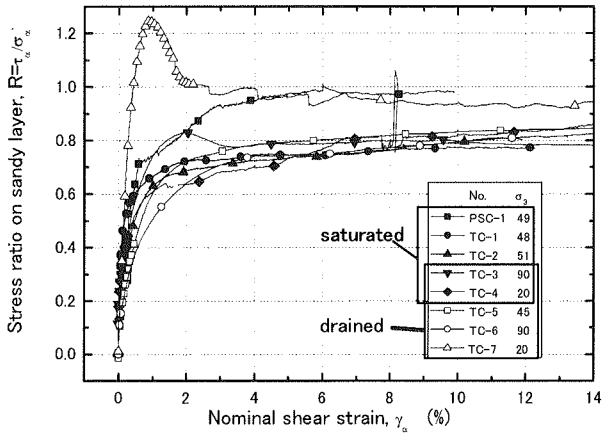

Figure 10. Stress ratio- shear strain relationships of undisturbed specimens

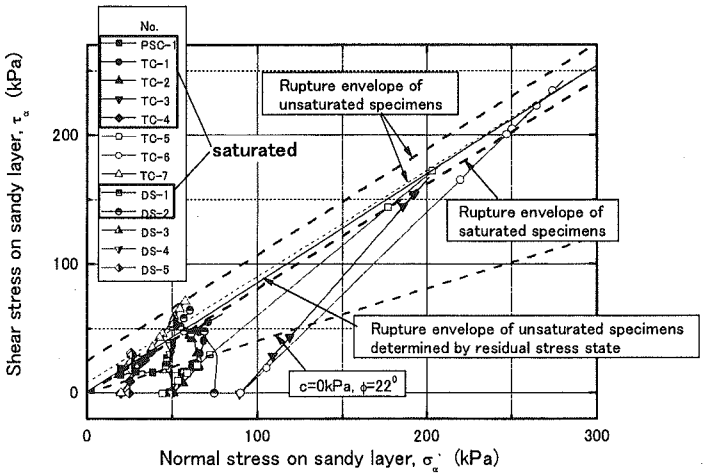

Figure 11. Relationships between normal stress and shear stress mobilized on weak layer of undisturbed specimen in PSC, TC and DC tests

In the case of unsaturated specimen, as the volumetric strain could not be measured, another

simplification is made by assuming that the volumetric strain was zero.

The test results are compared in **Figure 10** in terms of the relationships between $\tau_\alpha/\sigma'_\alpha$ and γ_α. Except for tests PSC-1 and TC-7, in all the tests the stress ratio of shear stress to effective normal stress on the sandy layer boundary was about 0.8 when γ_α exceeded 12%. The possible reason for the larger stress ratio in PSC-1 is that the test was a plain strain compression test and the confining plates restrained the deformation of the sandy layer in the σ_2 direction. In test TC-7, the sandy layer was denser than those of the other specimens. In addition, possible effect of apparent cohesion due to suction with the unsaturated specimen was more enhanced since the test TC-7 was conducted under lower effective confining stress (=20 kPa).

Figure 11 shows the relationship between normal stress and shear stress mobilized on the sandy layer of undisturbed specimens in PSC, TC and DC tests (Tsutsumi *et al.* 2007). All the peak stress states are below the envelope line $\tau = 24.9 + 0.82 \times \sigma'$. For this envelope, the following strength parameters are obtained: cohesion c=24.9 kPa and peak friction angle $\phi_{peak} = 39.4°$. In **Figure 11**, it was also attempted to distinguish the difference between the saturated and unsaturated specimens. As a result, the strength parameters as listed in **Table 2** were obtained.

Table 2. Strength parameters of the saturated and the unsaturated specimens

	ϕ_{peak} (deg.)	c_{peak} (kPa)		ϕ_{res} (deg.)	c_{res} (kPa)
Saturated specimens	39.0	0		-	-
Unsaturated specimens	39.4	maximum	minimum	40.2	0.9
		24.9	8.1		

As shown in **Figure 11**, the peak strength of the sandy layer is much larger than the condition of c=0 and $\phi = 22°$. This implies that the 22-degree slope would have been stable even after the heavy rain fall if the earthquake had not happened. The next step of this research is, therefore, to investigate the earthquake effect by applying cyclic loading.

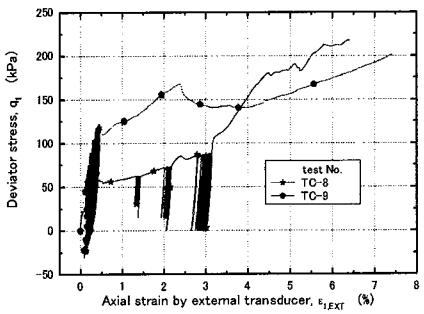

Figure 12. Stress-strain relationships of undisturbed samples in cyclic loading

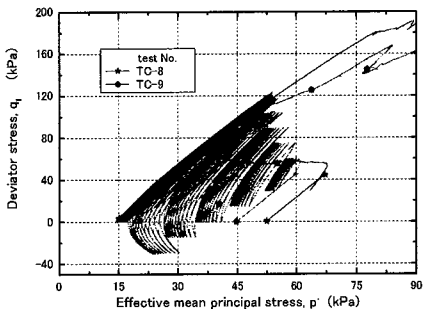

Figure 13. Stress paths of undisturbed samples in cyclic loading

Figures 12 and **13** show the cyclic loading test results. For specimen TC-8, when the axial strain exceeded 3% the stress-strain curve became very stiff because one of the two softrock blocks across the sandy layer touched both the top cap and pedestal. For specimen TC-9, two peaks can be found in **Figure 12**. A possible reason for these two peaks is that in the sandy layer, there were several relatively stronger sandy blocks; when two of them were crushed one by one, two peaks appeared

successively. Neither specimen TC-8 nor specimen TC-9 liquefied as shown in **Figure 13**. These results are possibly affected by the membrane compliance as described later in this paper.

Test results on artificial specimens

In order to study the possible effect of the thickness of sandy layer on its liquefaction characteristics, three tests were performed on artificial specimens.

Figures 14 and **15** show the test results on specimen A-1 which was made of Toyoura sand. Starting

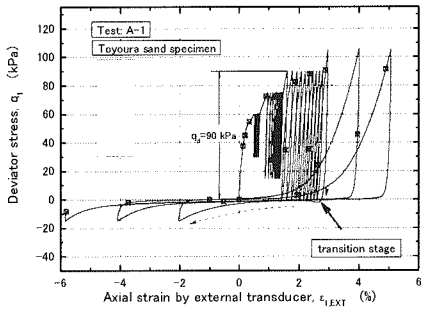

Figure 14. Stress-strain relationship of cyclic loading test A-1

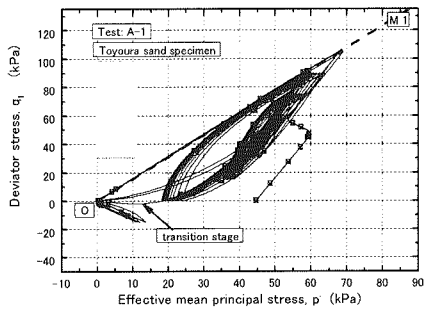

Figure 15. Stress path of cyclic loading test A-1

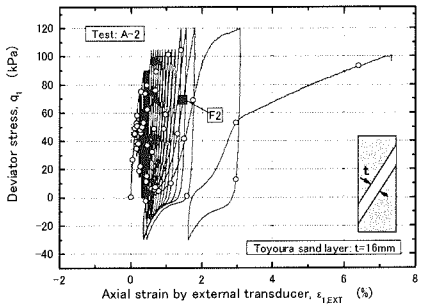

Figure 16. Stress-strain relationship of cyclic loading test A-2

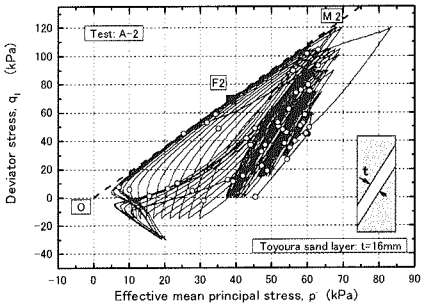

Figure 17. Stress path of cyclic loading test A-2

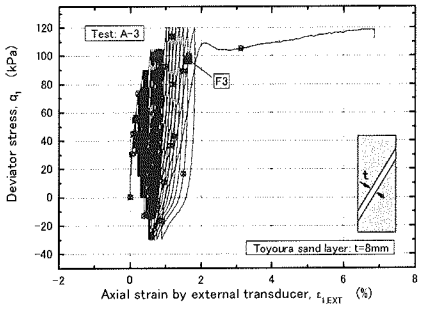

Figure 18. Stress-strain relationship of cyclic loading test A-2

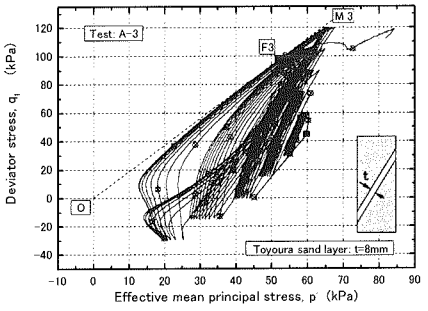

Figure 19. Stress path of cyclic loading test A-2

from the initial effective confining stress of 45 kPa and the initial deviator stress of 45 kPa, the specimen did not liquefy even after 10 cycles of undrained loading with double amplitude of deviator stress q_d =90 kPa. When the triaxial compression stress state was replaced by the triaxial extension stress state (i.e. $q_1 = \sigma_v - \sigma_h < 0$) for the first time, as shown by the arrow in **Figure 14**, the specimen deformed extensively. Only after another three cycles, the double amplitude vertical strain exceeded 10%. In the stress path shown in **Figure 15**, the zero effective stress state (i.e. $p' = 0$) was mobilized after the first transition stage from triaxial compression to triaxial extension during cyclic loading. These two facts confirmed that liquefaction did occur with this prismatic sand specimen.

Figures 16 and **17** show the test results on specimen A-2 which was made of 16-mm-thick Toyoura sand layer sandwiched by two softrock blocks. Though it was subjected to the same loading stages as specimen A-1, no large deformation occurred even when $q_1 \approx 0$ (**Figure 16**); and the stress path did not pass the origin (**Figure 17**) during all the loading cycles, therefore full liquefaction did not occur with specimen A-2. Similarly, with specimen A-3 which had an 8-mm-thick Toyoura sand layer, liquefaction did not occur either (**Figures 18** and **19**).

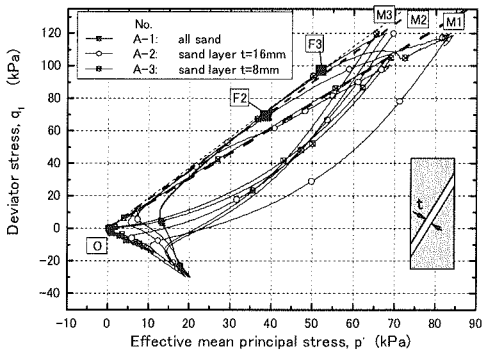

Figure 20. The last two cyclic loops of cyclic loading tests on artificial specimens

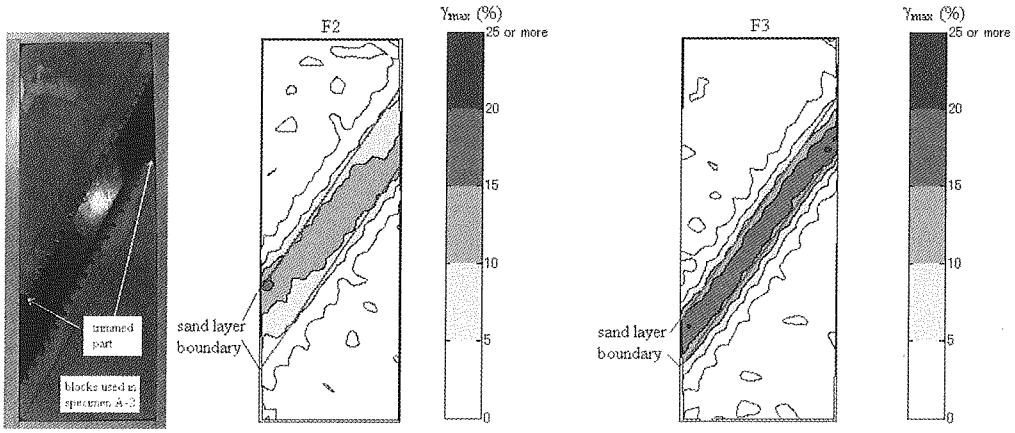

Figure 21. Maximum shear strain distributions at state F2 in test A-2 and F3 in test A-3

The possible reason for the above is that, because of the membrane compliance that will be described in this paper later, the sandwiched sand needs to expel at least 1 cm^3 water when the pore water pressure increases from the initial pore pressure of 200kPa to 245kPa in achieving the zero effective stress state. For specimen A-1, as it is fully made of sand, during shearing it can provide the

necessary magnitude of water deprived by member compliance when the pore water increases from the initial 200 kPa to 245 kPa, and it can achieve the zero effective stress sate. In contrast, the sandwiched sand in specimens A-2 and A-3 can not provide such amount of water as the quantity of sand is much less than in A-1, and the softrock blocks in these specimens can provide very limited amount of water as well, so the zero effective stress sate is not achieved.

Effective stress paths during the last two cyclic loops in these three tests are compared in **Figure 20**. The peak stress ratio envelope lines as denoted by OM1, OM2 and OM3 correspond to the results on specimens A-1, A-2 and A-3, respectively. **Figure 21** shows the maximum shear strain distribution at the state of peak stress ratio. It can be inferred that the sandwiched sand layer including its boundaries controlled the peak stress state. As the slopes of the envelope lines OM1, OM2 and OM3 in **Figure 20** are significantly different from each other, the mobilized friction angles of the sand layer have different magnitudes in the three tests. They become larger in the order of OM1, OM2 and OM3. Such difference in the mobilized friction angles is possibly related to the thickness of sand layer which

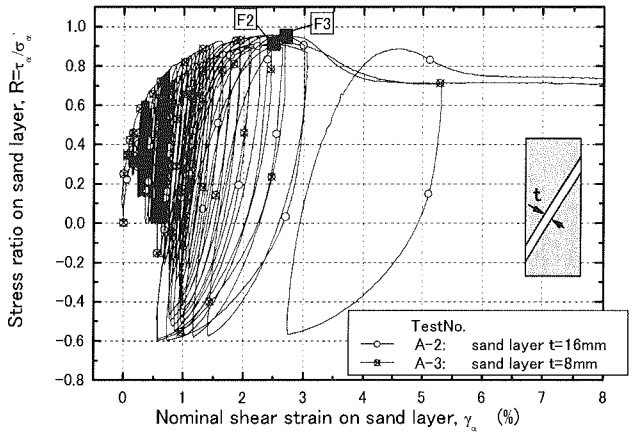

Figure 22. Stress ratio- shear strain relationships on sand layer of artificial specimens

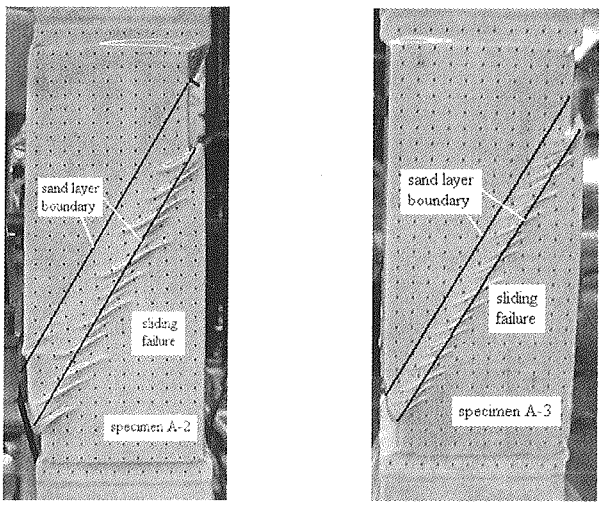

Figure 23. Sliding failure in artificial specimen

caused the different degrees of partial drainage (i.e. the different effective stress paths) as described later. Result from test A-3 with thinner sandy layer is affected by the highest degree of partial drainage. The present test results suggest, therefore, that the higher degrees of partial drainage result in larger angles of mobilized friction. Such behavior is consistent with the experimental observation reported by Kutter and Chen (1997) that the mobilized friction angle is dependent on the direction of the effective stress path.

Figure 22 shows stress ratio- shear strain relationships on the sand layer of artificial specimens A-2 and A-3. In this plot as well, the peak stress ratio mobilized on the sand layer is dependent on its thickness, which is achieved during the cyclic loop next to the last one. Finally, sliding failure occurred along the boundary between the sand layer and the softrock block as shown in **Figure 23**.

Test results on dummy specimen

As shown in **Figure 24**, results from three tests on dummy specimen showed that the space covered by membrane can expand by 1 cm^3 when the effective confining stress decreases from 45 kPa to 5 kPa. If liquefaction is to occur under nominally undrained condition, it is necessary that more than 1 cm^3 water shall be provided by the soil.

Such membrane compliance is affected by three factors at least. One factor is that the cross-section of dummy specimen (60x80 mm) is different from those of the top cap and pedestal (62x76 mm). The membrane is, therefore, wrinkled around the top and bottom edges of dummy, and the wrinkle will affect its inner space volume when effective confining stress changes. Another factor is that the dummy has four sharp corners having a right angle on its cross-section. When the effective confining stress is high enough, the membrane can touch tightly the dummy around these four corners as well as the other side surfaces. On the other hand, when the effective confining stress decreases, a small part of the membrane may separate from the dummy, and thus the inner space volume covered by the membrane will increase. The filter paper is likely to be the other factor. As filter paper is used in all the tests, its volume change due to the change of effective confining stress is inevitable.

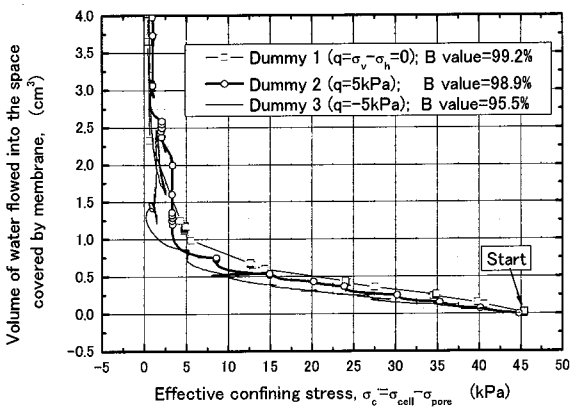

Figure 24. Membrane compliance

Because the volume of sandy layer in the undisturbed specimens is in the range of about 96 to 288 cm^3 and the volume of softrock parts change very little, the drained water due to the above membrane compliance by 1 cm^3 will cause volumetric strain of about 0.3%- 1% when effective confining stress decreases from 45 kPa to 5 kPa in nominally undrained test. So the undrained tests in this paper are actually partially drained tests, and liquefaction phenomena will be influenced significantly by such membrane compliance. For the three artificial specimens as reported earlier in this paper, the volume of partially drained water due to the decrease in the effective confining stress would be the same

among them, while the volume of sand layer is different from each other. Therefore, the partial drainage took place to different degrees; specimen A-3 has the highest degree of drainage and specimen A-1 has the lowest one.

CONCLUSIONS

The following conclusions can be drawn from the test results presented in this paper:

1) Softrock specimens without sandy layer had a peak strength of 3,000 kPa, while those with sandy layer had peak strength of 40-100 kPa under the effective confining stress of about 50 kPa in saturated tests. According to the image analysis results, deformation was localized in the sandy layer.
2) The peak and residual strengths of undisturbed specimen with the sandy layer were summarized. The peak strength of the sandy layer was much larger than the condition of c=0 and $\phi = 22^\circ$.
3) Dummy test and artificial specimen test results showed that membrane compliance can significantly affect the effective stress path during nominally undrained cyclic loading.

ACKNOWLEDGMENT

This study was conducted as a part of the research on "Earthquake damage in active-folding areas: Creation of a comprehensive data archive for remedial measures for civil-infrastructure systems" that is supported by Special Coordination Funds for Promoting Science and Technology of Japan Ministry of Education, Culture, Sports, Science and Technology.

REFERENCES

Ampadu, S.K. and Tatsuoka, F. (1993). "Effect of setting method on the behavior of clays in triaxial compression from saturation to undrained shear." *Soils and Foundations*, 33 (2), 14-34.

Kameya, H., Kanai T., Deng J., Tsutsumi Y. and Koseki J. (2006). "Retrieval of samples from a failed slope by Chuetsu Earthquake and their laboratory testing." *Proc. Japan National Conf. on Engrg. Geology in 2006*, JSEG, Kumamoto, pp.385-388 (in Japanese)

Kutter, B. L. and Chen, Y.-R. (1997). "Constant p' and constant volume friction angles are different." *Geotechnical Testing Journal*, Vol. 20, No.3, pp. 304-316.

Ministry of Land, Infrastructure and Transport (2005), "Information on the Chuetsu Earthquake." http://www.mlit.go.jp/kisha/kisha05/05/050113_.html (in Japanese).

Salas Monge, R. and Koseki,J. (2002). "Plane strain compression tests on cement treated sand." *Proceedings of the Fourth International Summer Symposium*, JSCE, Kyoto, pp. 223-226.

Tsutsumi Y., Deng J., Kameya H. and Koseki J. (2007). "Effect of weak layer on earthquake-induced failure of dip slope and site investigation techniques for its evaluation." *Symposium on the disaster prevention at active fold areas: scientific investigations, future research topics and suggestions of remedial measure on the disaster in 2004 Niigata-ken Chuetsu Earthquake*, JSCE, Tokyo, pp. 41-60 (in Japanese).